AN INTEGRATED HIGH-PERFORMANCE COMPUTING RELIABILITY PREDICTION FRAMEWORK FOR GROUND VEHICLE DESIGN EVALUATION

Dan M. Ghiocel
GP Technologies, Inc.
Pittsford, NY 14534

Dan Negrut
Mech. Engineering
Univ. of Wisconsin
Madison, WI

David Lamb
U.S. Army TARDEC
Warren, MI

David Gorsich
U.S. Army TARDEC
Warren, MI

ABSTRACT

This paper addresses some aspects of an on-going multiyear research project of GP Technologies for US Army TARDEC. The focus of the research project has been the enhancement of the overall vehicle reliability prediction process. This paper describes briefly few selected aspects of the new integrated reliability prediction approach. The integrated approach uses both computational mechanics predictions and experimental test databases for assessing vehicle system reliability. The integrated reliability prediction approach incorporates the following computational steps: i) simulation of stochastic operational environment, ii) vehicle multi-body dynamics analysis, iii) stress prediction in subsystems and components, iv) stochastic progressive damage analysis, and v) component life prediction, including the effects of maintenance and, finally, iv) reliability prediction at component and system level. To solve efficiently and accurately the challenges coming from large-size computational mechanics models and high-dimensional stochastic spaces, a HPC simulation-based approach to the reliability problem was implemented. The integrated HPC stochastic approach combines the computational stochastic mechanics predictions with available statistical experimental databases for assessing vehicle system reliability. The paper illustrates the application of the integrated approach to evaluate the relliability of the HMMWV front-left suspension system.

INTRODUCTION

An aspect of a key importance for accurate reliability prediction is the integration of various types of uncertain information sources and the incorporation of the lack of data effects. If modeling uncertainties are included, the stochastic dimensionality of the vehicle reliability problem increases from a single stochastic model to a set of stochastic prediction models that correspond to the stochastic model space. It should be noted that stochastic model space is usually a high-dimensional parameter space since it includes various model parameters that are considered random quantities. A flowchart of the computational reliability prediction process is shown in Figure 1 [3]. The paper focuses on the two upper-left blocks of the reliability chart that are drawn with dotted lines, that incorporate stochastic modeling and simulation of i) road profiles and ii) vehicle system dynamic behavior. However, for reader's clarity, we briefly discuss other important aspects of the vehicle reliability prediction. The two lower-level blocks called "TAO RBDO" that are a specific part of the reliability-based optimization process using the TAO software developed by Argonne National Lab that is not addressed in this paper.

The HMMWV suspension reliability analysis consisted in the following steps:

1) Simulate stochastic road profile variations. The idealization of road profiles includes the superposition of two stochastic variations: i) the road surface variation (micro-scale continuous, including smooth variations and random bumps or holes), and ii) the road topography variation (macro-scale continuous variations, including curves and slopes).

2) Simulate the HMMWV suspension parameters using randomly distributed variables to modify the nominal values. Average vehicle speed was varied between 17 MPH and 30 MPH.

3) Perform multibody dynamics simulations of the HMMWV system using as stochastic inputs the road profiles and vehicle suspension dynamic parameters (stiffness, damping). For each simulated road profile, an ADAMS vehicle multibody dynamics analysis is run to get simulated forces and displacements at each joint of the suspension system.

4) Perform finite element (FE) stress analysis of the selected subsystem. From each HMMWV dynamics simulation a number of local response variables were considerd as random inputs for the stochastic FE stress analysis of the Front-Left Suspension System (FLSS). An efficient high-performance computing (HPC) stochastic finite-element analysis (FEA) code, specifically developed by GP Technologies for TARDEC, is employed.

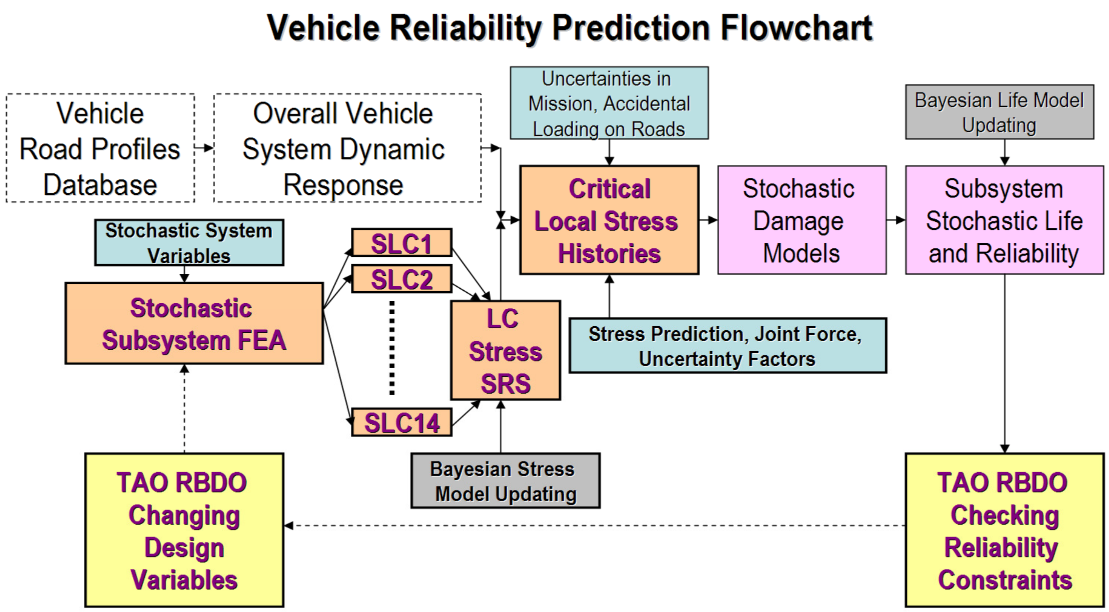

Figure 1 Vehicle reliability prediction flowchart [3]

5) Compute the local stresses refined using stochastic response surface approximation (SRSA) models. These SRSA models are based on high-order stochastic field models that are capable of handling non-Gaussian variations, and non-linear correlations between component variables.

6) Perform durability analysis under random corrosion-fatigue damage using stochastic crack nucleation and crack propagation models based on the damage curve approach (DCA) and the modified Forman crack propagation models. For reliability prediction at each critical location, probabilistic models based on lognormal and Weibull distributions were applied.

7) Incorporate the uncertainty effects due to the lack of data.

8) Incorporate Bayesian updating models for including experimental evidence form test data (for stresses) and field data (field failures).

The paper provides in next sections more details on the reliability prediction methodology and, also, illustrates HMMWV sensitivity analysis results. It should be noted that the presented results are based on a “modified” HMMWV vehicle model developed based on incomplete, limited published information [2].

OPERATIONAL ENVIRONMENT

This section briefly describes the stochastic models used for the simulation of the road profiles.

The idealization of road profiles includes the superposition of two stochastic variations: i) the road surface variation (micro-scale continuous, including smooth variations and random bumps or holes), and ii) the road topography variation (macro-scale continuous variations, including curves and slopes). The idealization of road profiles includes the superposition of two stochastic variations: i) the road surface variation (micro-scale continuous, including smooth variations and random bumps or holes), and ii) the road topography variation (macro-scale continuous variations, including curves and slopes). Vehicle suspension parameters were varied by using randomly distributed variables to modify the nominal values. Average vehicle speed was varied between 17 MPH and 30 MPH. Simulations were run using random combinations of the above mentioned variations.

Specifically, we idealized the road surface profiles as non-Gaussian, non-stationary vector-valued stochastic field models with complex spatial correlation structures. To simulate stochastic road profiles, we idealized them by non-Gaussian, non-stationary Markov vector processes that were obtained by solving a set of nonlinear, stochastically coupled second-order differential equations. The nonlinear mapping is based on an algebraic probability transformation of real, non-Gaussian variations defined by the available databases for road surfaces and topography to an ideal Gaussian image space.

Figure 2 shows simulated road surface segments with high spatial correlation (HC) and low spatial correlation (LC) in the transverse direction of the road. The longitudinal variation of the mid-line road surface profile is the same for both HC and LC simulated roads. The HC road corresponds to a situation when the wheel inputs are about the same for two parallel wheel lines, so that right-side and left-side wheels see about the same road surface track lines. Thus, for the HC roads, there two different wheel road inputs, each input for a pair of front-rear wheels. In contrast, the LC road assumes that the right-side and left-side wheel road inputs are different. Thus, for LC roads there are four different wheel inputs. Thus, it is expected that a LC road profile will produce slighly larger vehicle dynamic responses in all directions, especially in the lateral direction.

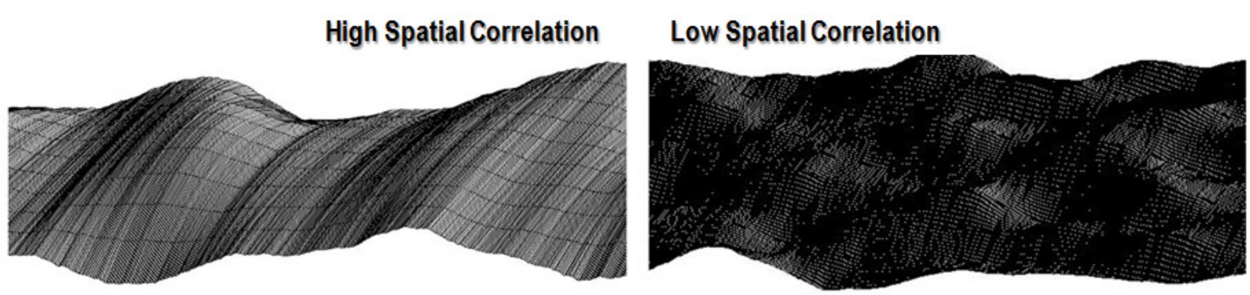

Figure 2 Simulated road surfaces with high (left) and low (right) transverse spatial correlations

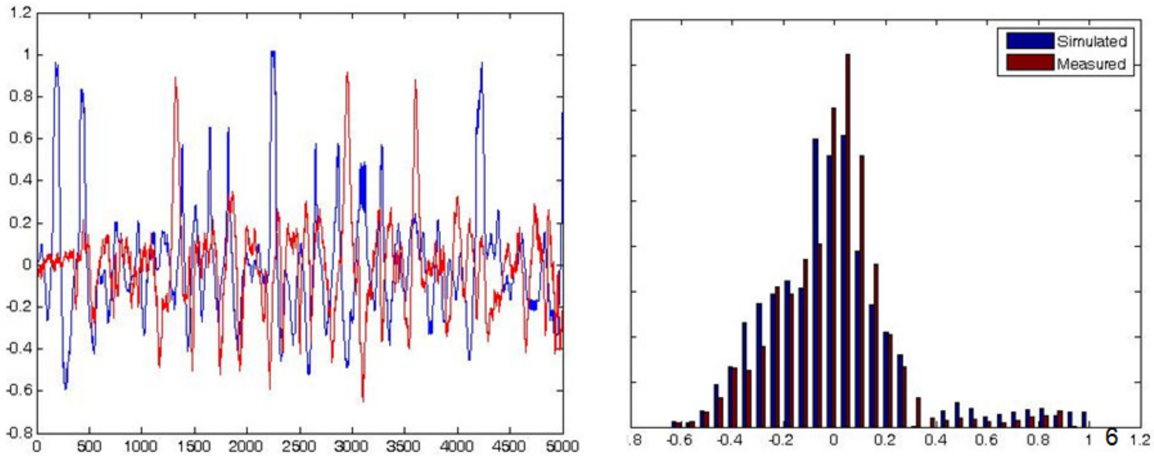

Figure 3 Simulated (blue) and measured (red) road profiles (left plot) and their PDF (right plot)

Based on various road measurements we noted that the road surface variations are highly non-Gaussian as shown in Figure 3. This is somehow surprising since in the current practice the road surface profiles have been always idealized by simple zero-mean Gaussian stationary stochastic processes. For Gaussian stochastic processes, the covariance function (CF), or, alternatively, the power spectral density function (PSD, fully describes the stochastic process variation. In practice, the RMS value (standard deviation) and the PSD estimate are often used. Unfortunately, the RMS and PSD estimates are not sufficient for describing the non-Gaussian road surface variations. Most of the times, the road surface variations are highly non-Gaussian variations with a highly skewed probability density function (PDF) as indicated in Figure 3. The non-Gaussian variation aspect has a significant impact on the vehicle fatigue reliability prediction. It should be noted that if the non-Gaussian variation aspects of road surfaces are neglected, then, the predicted vehicle fatigue life and reliability are much larger than in reality.

Figure 4 shows simulated non-Gaussian stochastic road surface profiles (median line) with different road roughnesses and no topography included. These segments correspond to limited-size stationary segments of the road profiles.

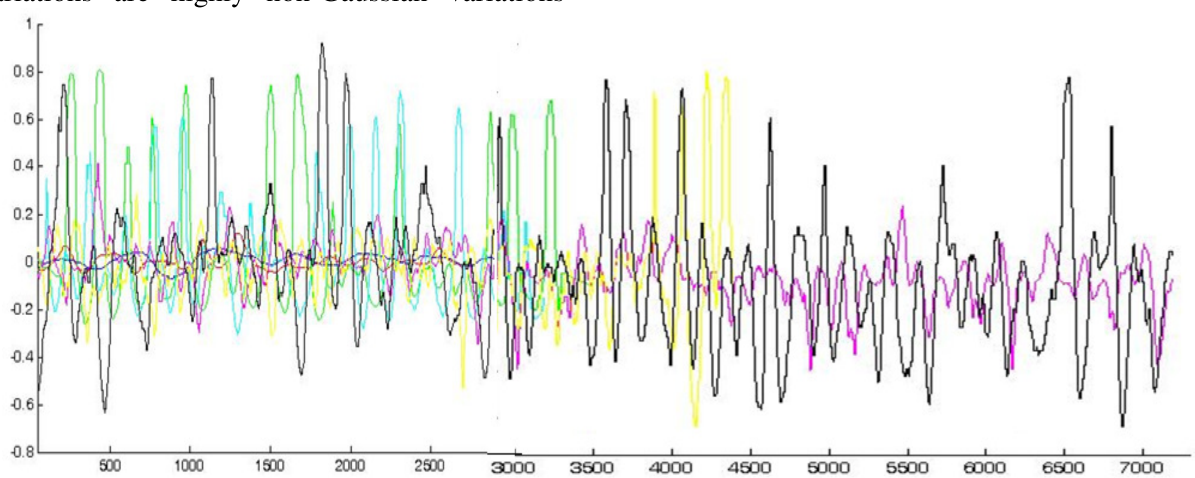

Figure 4 Simulated road profiles (stationary segments) for different road roughnesses

VEHICLE DYNAMIC MODEL

Specifically, in this project the HMMWV model number M966 (TOW Missle Carrier, Basic Armor without weapons) was selected, since the values of the total vehicle inertia were available [2]. The HMMWV vehicle is designed for both on-road and off-road applications, and all models share a common chassis with 4x4 wheel drive that is powered by a 145-hp engine. Only the major subsystems which were included in the HMWWV dynamic model (Figure 5) including parallel link steering with a pitman arm, double A-arm suspension, chassis, roll stabilization bar, powertrain and tires. Subsystems for the brakes and wheels were also included in the multi-body dynamics model.

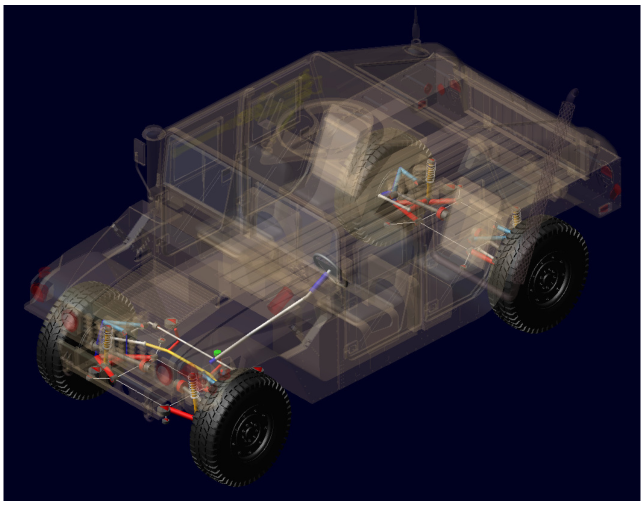

Figure 5 ADAMS HMMWV Dynamic Model

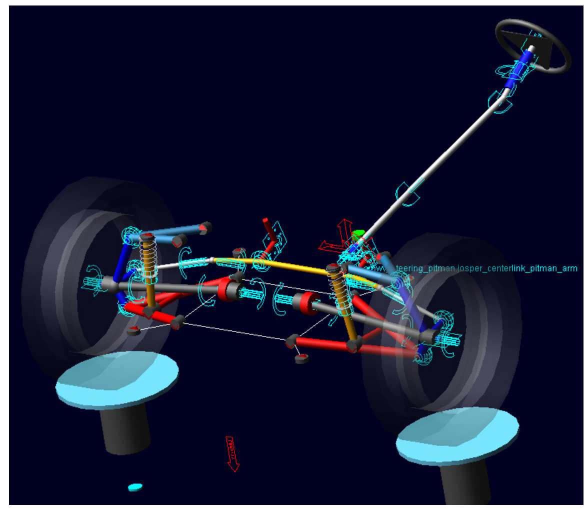

Figure 6 ADAMS Front Suspension Model

A double Ackerman Arm type suspension unit is used on the HMMWV, one for each wheel. Dimensions and locations of the suspension elements differ between the front and rear subsystems; however, the topology remains the same. Both upper and lower control arms are connected to the upright arm with ball joints. The upright arm connects the wheel spindle to the suspension units. Rear radius rods are connected between the chassis to the rear suspension and control the rear wheel static toe angle. Front tie rods attach the steering subsystem with the front suspension and control the wheel steer angle. Front and rear suspensions both have a design Kingpin angle of 12 degrees and a kingpin offset of 2.14 inches. The front suspension has a caster angle of 3 degrees and a caster offset of 0.857 inches. Topology of the suspension as modeled in ADAMS/Car can be seen in Figure 6.

Shock absorber units are located on each suspension unit, and are attached between the lower control arm and chassis. Each shock absorber is comprised of three elements: a spring, a damper and a bumpstop. At design load and height, the springs are assumed to have linear behavior. The dampers on the other hand are meant to provide dissipative forces and are not linear. Dissipative forces are proportional to the relative velocity between the piston and cylinder of the shock. Both front and rear springs and dampers were modeled in a similar way, but using different data.

The rear springs and dampers are designed for larger operating loads. Bumpstops are located on the end of the damper and provide an additional damping force in the shocks. They are engaged only after a certain amount of displacement occurs between the piston and cylinder of the shock absorber. Spring, damper and bumpstop parameters can be found in [2].

The vehicle body is modeled as a single rigid-body component with mass-inertia properties as given in [2]. As stated earlier, both the vehicle mass-inertia properties and the masses of the individual subsystems are known. Simplified geometry like that in Figure 4 was used to calculate each subsystem's respective moment of inertia values.

Tires used for all simulations were the Goodyear bias-type 36x12.5 LT Wrangler II. Front tire pressures of 20 pounds per square inch (psi) and rear tire pressures of 30 psi were maintained on the HMMWV. By using FTire's template modeling scheme [1], only a select number of tire size, geometry and specification parameters were needed as input into the tire model; other characteristics such as carcass mass/damping/stiffness, tread and friction information were either inherited from the light truck tire template or could be calculated with FTire's pre-processor routine.

A more detailed description of the HMMWV ADAMS model is provided elsewhere [7].

HMMWV BEHAVIOR SIMULATION

In light of the importance of the tire/road interaction due to the stochastic modeling of the road profiles, a co-simulation environment was used to accurately capture the vehicle dynamics. The MSC ADAMS/Car code was used to simulate the multi-body dynamics of the vehicle, and the tires and tire/road interaction are simulated by FTire. Road profiles of nearly a mile in length were used, and as such the computational model for determining the tire/road forces must be efficient and scalable.

ADAMS/Car is a complete vehicle simulation package distributed by MSC. Software and in this work it is used to investigate the behavior of the rigid multi-body model of HMMWV. The modeling methodology divides a vehicle in subsystems that are modeled independently. Parameters are applied to the topology of a subsystem and a set of subsystems are invoked and integrated together at simulation time to represent the vehicle model. The subsystems present in our model include: a chassis, front and rear suspension, anti-roll bar, steering, brakes, a powertrain and four wheels. Note that only the wheels and not the tires are present in the ADAMS/Car model. Also, all the major subsystems (front/rear suspension, steering, roll bar and powertrain) are connected to the chassis with bushing elements. The HMMWV model as seen in ADAMS/Car is shown in Figure 5 (chassis geometry is partially transparent). CAD geometry is applied to the chassis and tires to make the vehicle look realistic for animation purposes. The geometry has no bearing on the dynamic behavior of the vehicle.

Driver controls were created in the ADAMS/Car event builder as a sequence of maneuvers. Maneuvers are defined by steering, throttle, brake, gear, and clutch parameters. In this set of simulations, a single maneuver is performed in which the vehicle attempts to follow the centerline of the road profile at a given vehicle speed. Static set-up and gear shifting parameters are not modified; however, the drive authority is sometimes reduced when large obstacles and high vehicle speeds cause simulations to fail. Drive authority specifies how aggressively the vehicle steering torque is applied when the vehicle deviates off the specified path. As the wheelbase of the HMMWV is wide and long, the minimum preview distance was substantially increased from its default value.

A number of about 500 stochastic simulations were performed assuming as stochastic inputs different road profiles and vehicle suspension parameters. Figure 7 decribes different categories of stochastic road profiles.

First, only the stochasticity associated to the road profile and vehicle speed were considered, assuming a deterministic HMMWV model. These simulations utilized the same vehicle/tire models, and varied the operating environment by changing 1) road profiles 2) adding topology and 3) modifying the average vehicle speed. Road profiles were either 5000 feet or 1500 feet in length, with both high and low correlation variations in the transverse direction. Topology on the road included rolling hills with short chicanes, long winding curves or no topology at all (straight road). The average vehicle speed was either 17 MPH or 30 MPH.

Secondly, for selected road profiles, we considered that the HMMWV model suspension parameter variations are stochastic. Two types of simulated road profiles with and without topographic effects were employed. For each wheel suspension system there are 13 random variables. For four wheel suspensions there are 52 variables. To handle these large numbers of variables we condensed them in three stochastic variation features: 1) BUSHINGS UCA (4 variables), 2) BUSHINGS LCA (4 variables), 3) TIRE (3 variables) and 4) SPRING-SHOCK ABSORBER (2 variables).

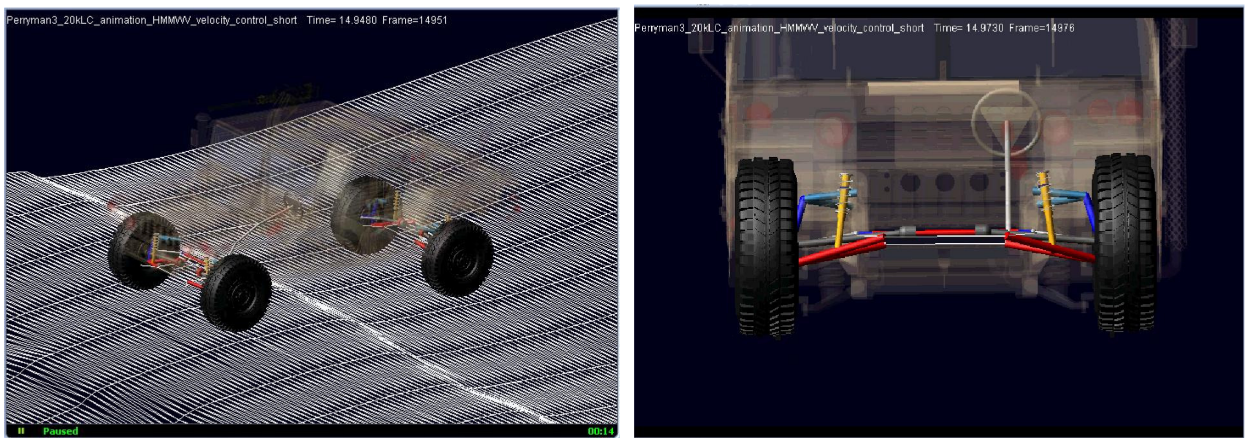

a) Flat road with no topography Effects; Passing a Random Bump

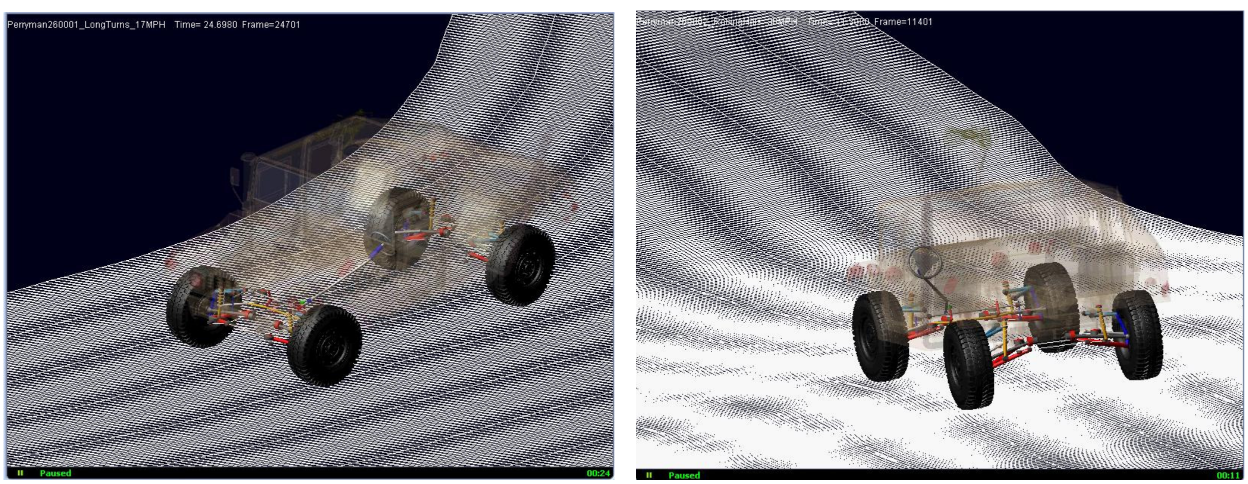

b) With topography Effects; Smooth and Rough Stochastic Roads

Figure 7 HMMWV Simulations with Stochastic Road Profiles

The stochastic variables are modeled by i) lognormal variables with 2% and 5% c.o.v. for the spring and damper properties, ii) lognormal variables with 2% c.o.v. for bushing properties, iii) lognormal variables with 5% c.o.v. for tire properties. Currently, we are still reviewing technical literature to find specific statistical information for HMMWV dynamic system parameters. Any specific information on HMMWV coming from TARDEC will be highly appreciated.

To simulate the four stochastic variation features, we used Latin Hypercube Sampling (LHS) technique. Using LHS, stochastic input scenarios were created for each vehicle suspension stochastic feature. For each of the four stochastic features we have simulated a number of 80 input scenarios that we run separately.

For each simulated road profile, we performed an ADAMS/Car vehicle multibody dynamics analysis to get forces and displacements at each joint of the front suspension system. Stochastic variations in vehicle dynamic parameters (stiffness, damping) were included. From each the vehicle dynamics simulation, we saved 34 output variables with 1-3 component time-histories for various front-left suspension joint forces and displacements, vehicle chassis motion, displacements at wheel tire/road interface.

A number of 36 variables were used as random inputs in the stochastic FE stress analysis of FLSS. Each joint force component was used to scale the local stress influence coefficients computed for unit forces in the joints.

SUSPENSION SYSTEM STRESS ANALYSIS

The stochastic subsystem stress analysis is based on an efficient high-performance computing (HPC) stochastic finite-element analysis (FEA) code implemented by GP Technologies. The developed HPC stochastic FEA code is called Stochastic PARallel Tool for Analysis for Computational Unstructure-meshed Solids or condensed SPARTACUS. Figure 8 shows the FLSS model used for the HMMWV ADAMS vehicle multi-body dynamics analysis and the stochastic FEA using SPARTACUS.

The SPARTACUS code is a result of integrating a finite element with a number of modules used for stochastic modeling and simulation that run together in an efficient computing environment driven by advanced HPC numerical libraries available from national labs and top universities. In addition to the standard FEA and HPC algorithms, SPARTACUS includes a unique suite of computational tools for stochastic modeling and simulation and stochastic preconditioning [3].

For stochastic FEA domain decomposition we used ParMETIS, an efficient multilevel partitioner software package developed by the University of Minnesota. Multilevel partitioners rely on the notion of restricting the fine graph to a much smaller coarse graph, by using maximal independent set or maximal matching algorithms. This process is applied recursively until the graph is small enough that a high quality partitioner, such as spectral bisection or k-way partitioners, can be applied. This partitioning of the coarse problem is then "interpolated" back to the finer graph – a local "smoothing" procedure is then used, at each level, to locally improve the partitioning. These methods are poly-logarithmic in complexity though they have the advantage that they can produce more refined partitions and more easily accommodate vertex and edge weights in the graph.

The main idea to build a flexible HPC implementation structure for stochastic parallel FEA has been to combine the parallel decomposition in the simulated sample data space with the parallel decomposition in the physical-model space. This combination of parallel data space decomposition with parallel physical space decomposition provides a very high numerical efficiency for handling large-size stochastic FE models. This HPC strategy provides an optimal approach for running large-size stochastic FE models. We called this HPC implementation is called the Controlled Domain Decomposition (CDD) strategy. The CDD strategy can be applied for handling multiple FE models with different sizes that will be split on a different number of processors as shown Figure 9. There is an optimum number of processors to be used for each FE model, so that the stochastic parallel FEA reaches the best scalability. The main advantage of the CDD implementation for HPC FEA is that large-size FE models can be partitioned into a number of FE submodels, each being solved on a single processor. Thus, each group of processors is dedicated to solve a large-size FE model. CDD ensures dynamic load balancing after a group of processors has completed its allocated tasks and it becomes available for helping another group of processors.

To be highly efficient for large-size FEA models, SPARTACUS incorporates an unique set of powerful stochastic preconditioning algorithms, including both global and local, sequential preconditioners. The role of preconditioning is of key significance for getting fast solutions for both linear and nonlinear stochastic FEA problems. It should be noted that the effects of stochastic preconditioning is larger for nonlinear stochastic FEA problems since it reduces both the number of Krylov iterations for linear solving and the number of Newton iterations for nonlinear solving. The expected speed up in SPARTACUS coming from stochastic preconditioning is at least 4-5 times for linear FEA problems and about 10-15 times for highly nonlinear FEA problems.

To compute local stresses in subsystem components, refined stochastic response surface approximation (SRSA) models are used. These SRSA models are based on high-order stochastic field models that are capable of handling non-Gaussian variations [4,5]. The SRSA implementations were based on two and three level hierarchical density models as shown in Figure 10. It should be noted that these SRSA models are typically more accurate than traditional responses surfaces, and are also limited to the mean response surface approximation.

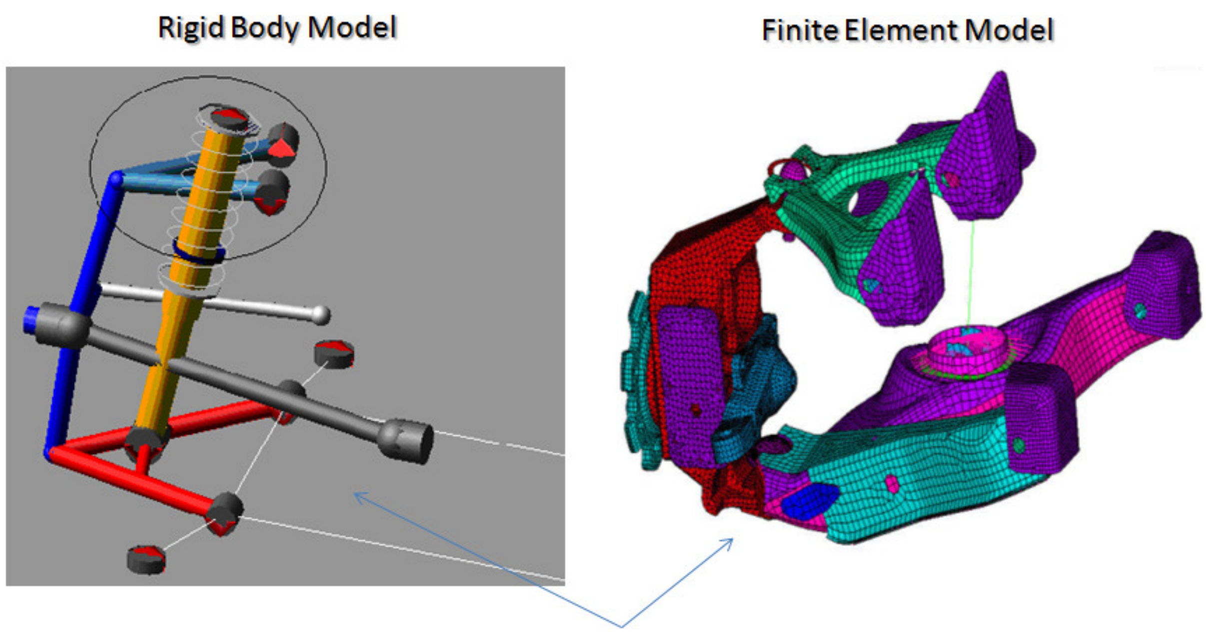

Figure 8: Front-Left Suspension System (FLSS); ADAMS model (left), and FEA model (right)

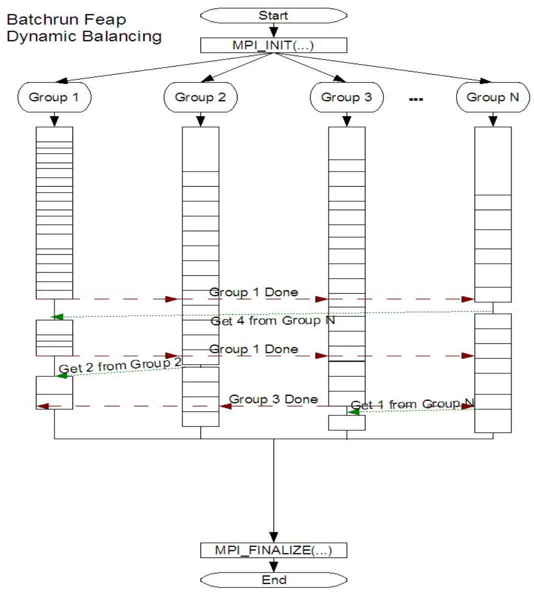

Figure 9 HPC CDD Implementation Strategy

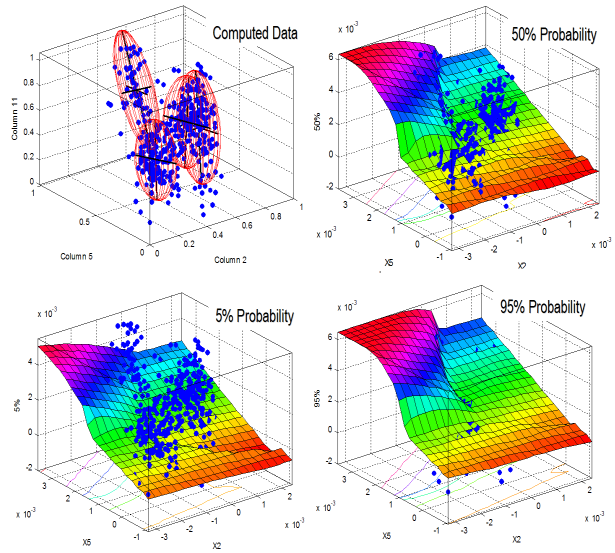

Figure 10 Stochastic Surface Approximation

PROGRESSIVE DAMAGE MODELS

For fatigue damage modeling, the following models are considered:

Crack Initiation: Stochastic Phenomenological Cumulative Damage Models:

1) Linear Damage Rule (Miner's Rule)
2) Damage Curve Approach (NASA Glenn)
3) Double Damage Curve Approach (NASA Glenn)

Crack Propagation: Stochastic Linear Fracture Mechanics-based Models:

1) Modified Forman Model (NASA JPC)

Both the constitutive stress-strain equation and strain-life curve are considered to be uncertain. The two Ramberg-Osgood model parameters and the four strain-life curve (SLC) parameters are modeled as random variables with selected probability distributions, means and covariance deviations. We also included correlations between different parameters of SLC. This correlation can significantly affect the predicted fatigue life estimates. We combined rainflow cycle counting with the Neuber's rule for local plasticity modeling for any irregular stress-strain history. For a sequence of cycles with constant alternating stress and mean stress the Damage Curve Approach (DCA) and Double Damage Curve Approach (DDCA) were implemented.

In comparison with the linear damage rule (LDR) or Miner's rule, these two damage models predict the crack initiation life much more accurately. The shortcoming of the popular LDR or Miner's rule is its stress-independence, or load sequence independence. LDR is incapable of taking into account the interaction of different load levels, and therefore interaction between different damage mechanisms or failure modes.

There is substantial experimental evidence that shows that LDR is conservative under completely reversed loading condition for low-to-high loading sequences, and severely under conservative for high-to-low loading sequence. For intermittent low-high-low-high-…cyclic loading, the LDR severely underestimates the predicted life. The nonlinear damage models, DCA and DDCA, were implemented to adequately capture the effects of the HCF-LCF interaction and corrosion-fatigue damage for vehicle subsystem components.

Crack propagation was implemented using a stochastic modified Forman model. Both the stress intensity threshold and material toughness are considered as random variables. Corrosion–fatigue damage effects due to pitting growth were considered by implementing a simultaneous corrosion-fatigue (SCF) model [4]. The total corrosion-fatigue damage in the crack nucleation stage is computed using a generalized interaction curve between corrosion and fatigue damages, while the in crack propagation stage is computed by linear fracture mechanic models (Forman model) for which the stress intensity factors are adjusted based on local crack size including both the fracture crack and the pit depth.

RELIABILITY PREDICTION

For life and reliability prediction we considered probabilistic life prediction models based on lognormal and Weibull probability distributions. To include the effect of the limited number of stochastic FEA simulation runs on the FLSS reliability we used both parametric and non-parametric bootstrapping techniques.

We also considered, as an option, the effect of off-line maintenance activities that include uncertainties related to the maintenance schedule, crack detection and sizing (Figure 11), and also the damage repair efficiency.

Typically, reliability is quantified by probability of failure. The failure is defined by either reaching the ultimate crack length or reaching the stress intensity crack stability limit. If maintenance effects are considered, then, the reliability metric of interest is the hazard failure rate (HFR) instead of the probability of failure that is defined as the probability of failure per unit time. Average HFR are computed for each maintenance interval between two scheduled maintenance events. A probabilistic mixture model with lognormally distributed components is used for reliability prediction when maintenance is considered.

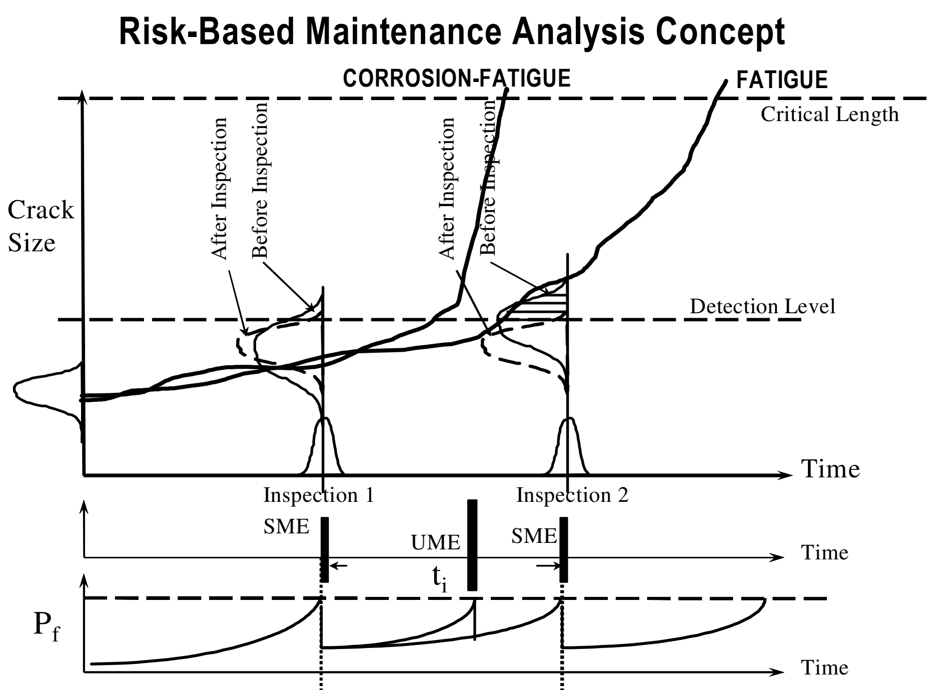

Figure 11 Reliability Prediction including Effect of Maintenance Activities

SENSITIVITY STUDY RESULTS

In this section we present selected results of several sensitivity studies. The output variables are considered the vehicle dynamic response and the local stresses at critical locations, predicted lives and reliability of FLSS for different stochastic input scenarios.

Firstly, we focus on the effect of the stochastic road profile non-Gaussianity. Figure 12 shows the FLSS responses for a Gaussian and a non-Gaussian straight, moderate roughness road profiles for a vehicle speed of 30 mph. The Gaussian and non-Gaussian road profiles have the same second-order statistical moments or power spectral densities. It should be noted that the local stress cycles at a critical location in LCA have about twice larger maximum amplitudes for non-Gaussian profile than for Gaussian profile. For different critical locations within FLSS, the predicted life is about 4 to 40 times shorter for non-Gaussian profile than for Gaussian profile. These results infirm the current practice that is based on the use of Gaussian process models for road profile idealization.

Next, we considered the effect of the road profile topography on the FLSS stress and life. We considered three types of simulated road profiles: i) straight profile (S) with a bump, ii) horizontally curved profile (long turns, LT) and iii) sloped and curved profile (rolling hills, RH). Figure 13 shows the effect of topography for a moderate roughness road profile on the FLSS joint forces. It should be noted that the effect of topography is important. The FLSS joint forces have several times larger amplitudes if topography effects are included.

Figures 14 and 15 show the FLSS LCA ball joint lateral force variation and, respectively, the local Von-Mises stress variations (history and stress range) and the associated rainflow matrix (in alternating strain and mean stress coordinates) at a critical location in the FLSS LCA system.

It should be noted that the maximum stress variation at the selected critical location is about ten times larger for the road profile with topography variation than for the straight road profile, although the road surface roughess is high for the simulated segment considered. For the S profile the maximum stress range amplitude is about 0.50 units if the bump is excluded, while for the RH profile the maximum stress range amplitude is about 5.30 units, and for the LT profile is 3.60 units.

Figure 16 shows the effect the progressive damage modeling on the FLSS life prediction. The linear damage rule (LDR) provides a life that is twice as long as the predicted life using a nonlinear damage rule such the damage curve approach (DCA). These results show that the unconditional use of LDR for any fatigue damage modeling could produce crude reliability analysis results. It should be noted that the two progressive damage models LDR and DCA for creack nucleation were combined with the stochastic Forman model for crack propagation [4].

Figure 17 illustrates the effect of lack of data, for 280 stochastic FEA simulations, on the probabilistic life prediction at a critical location of the FLSS LCA system. Both Weibull and lognormal life probabilistic models were considered. It should be noted that Weibull life model provides much shorter predicted lives for a given reliability level. For 99% reliability level, the mean Weibull life is 300 units in comparison with the mean lognormal life that is 750 units. This conservatism of the Weibull probablistic model is one important reason of the popularity of these models for life prediction in engineering practice.

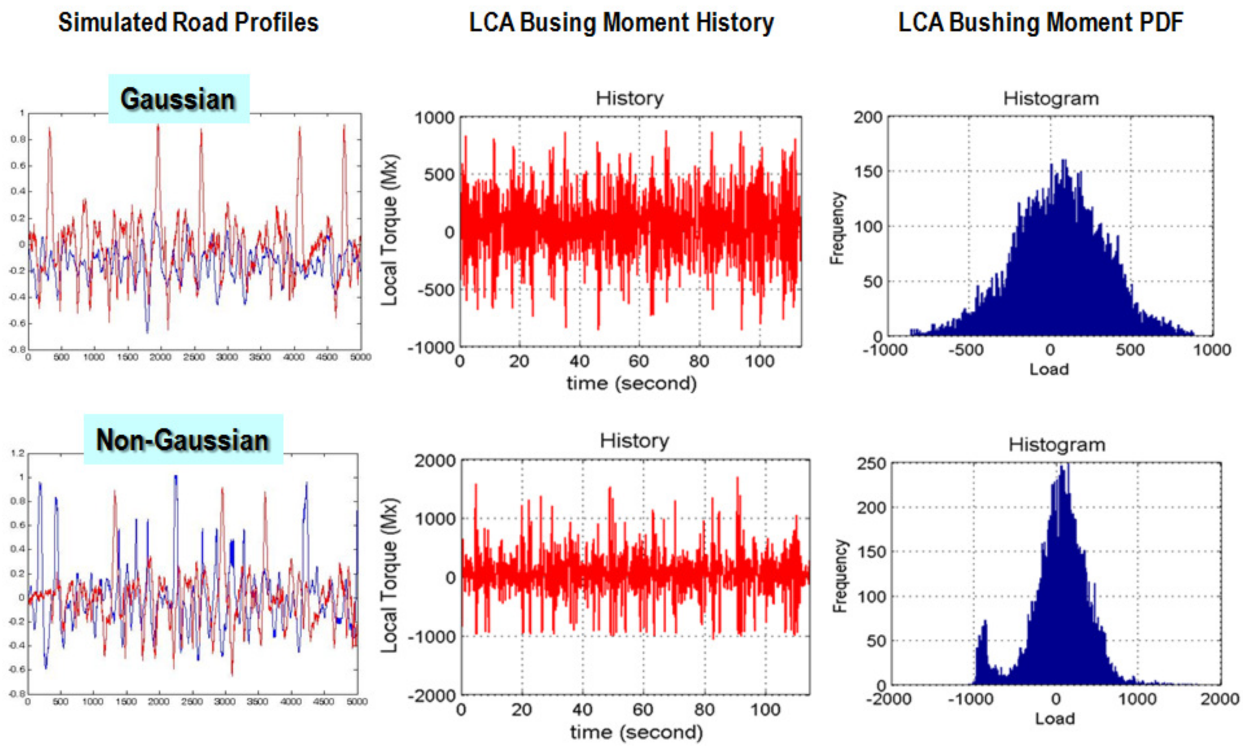

a) Measured and Simulated Road Profiles, Gaussian and Non-Gaussian, and Associated LCA Bushing Torque Moment Histories and PDF Estimates

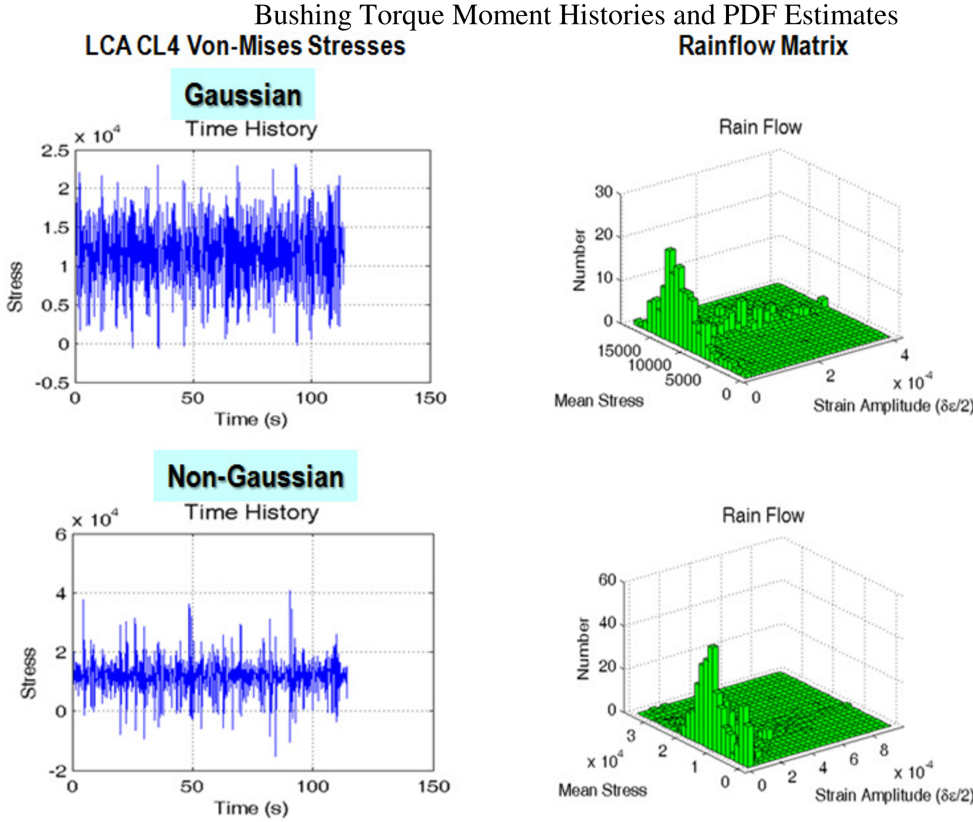

b) Simulated Local Stress Histories and Rainflow Matrices at A Critical Location in LCA

Figure 12 Vehicle FLSS Response for Gaussian and Non-Gaussian Road Profiles at 30 mph

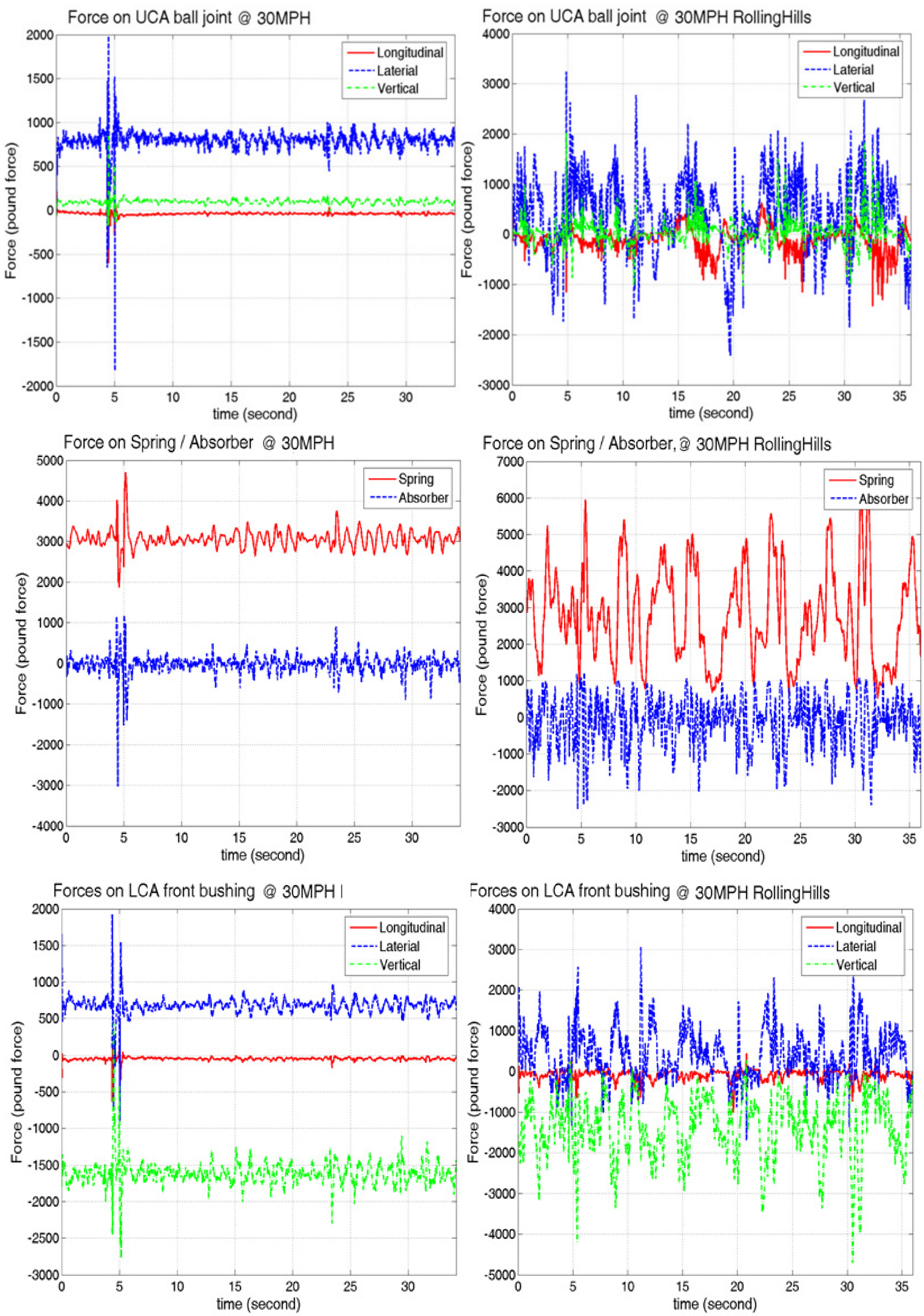

Figure 13 Joint Force Histories for S Profile (no topography) and RH Profile (with topography)

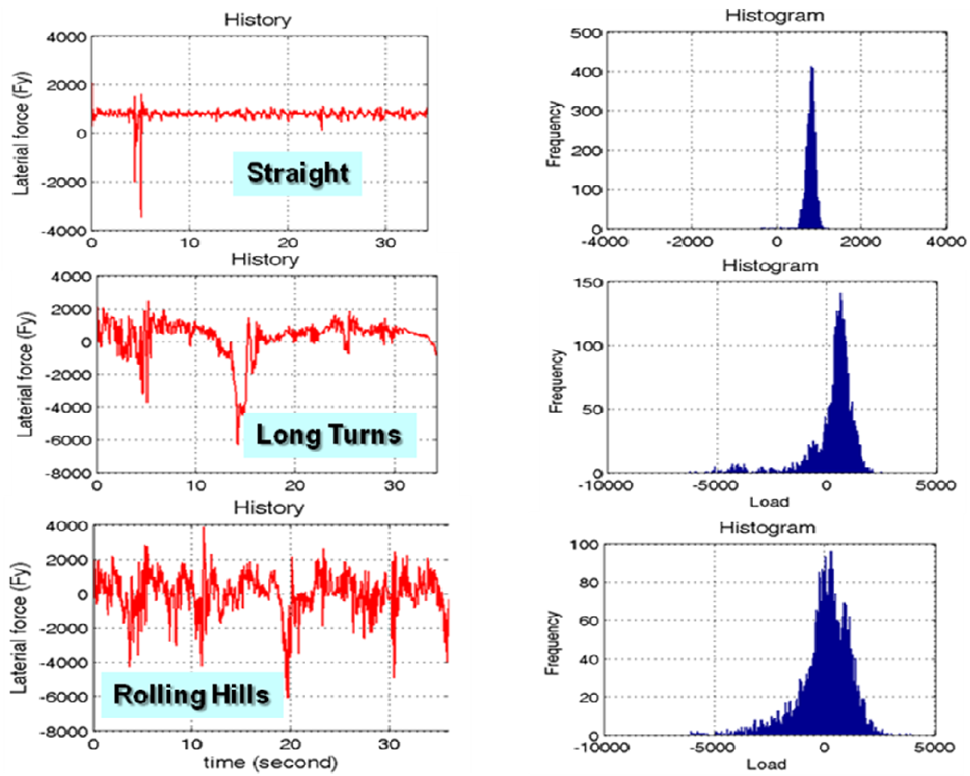

Figure 14 Joint Force Variations (Histories and PDF) in the LCA Ball Joint for Straight Road (upper), Horizontally Curved Road – Long Turns (middle) and Sloped and Curved Road – Rolling Hills (lower)

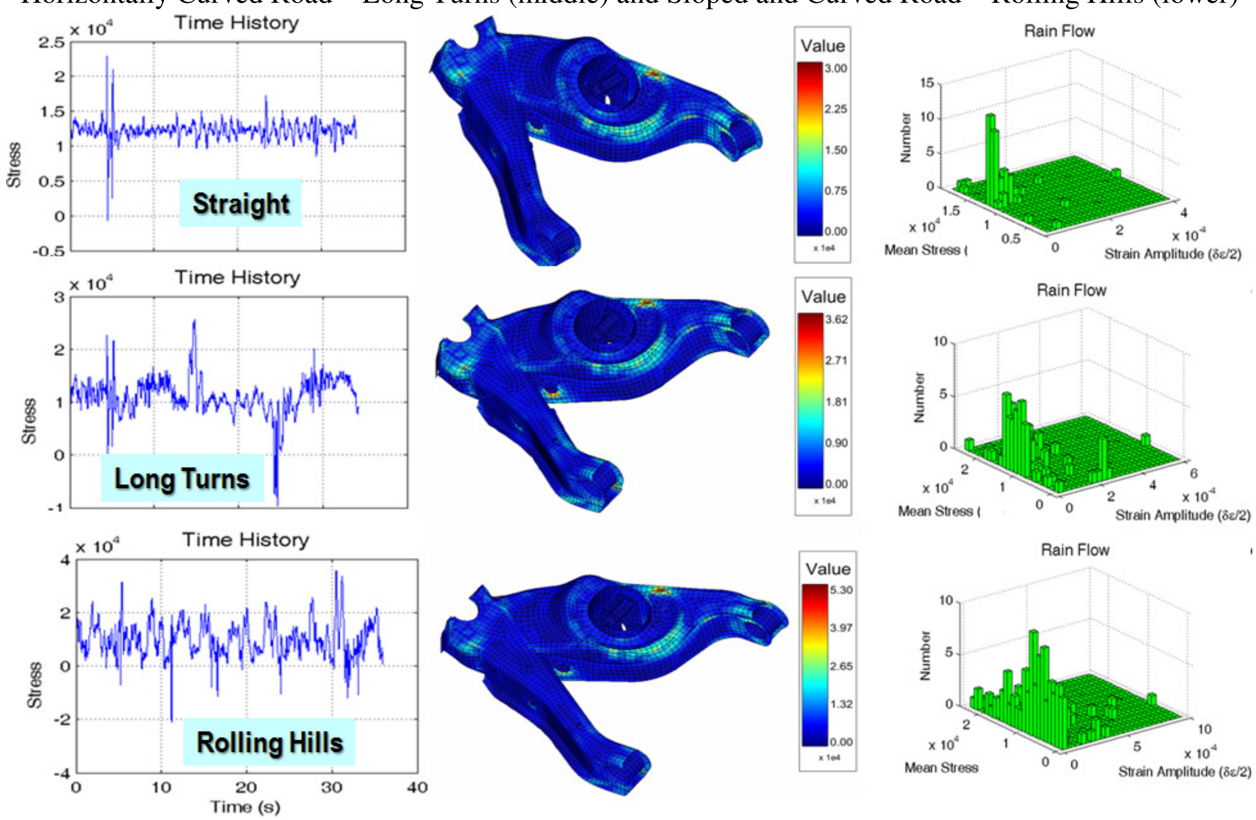

Figure 15 FLSS Stress at A Critical Location in LCA for Straight Road (upper), Horizontally Curved Road – Long Turns (middle) and Sloped and Curved Road – Rolling Hills (lower)

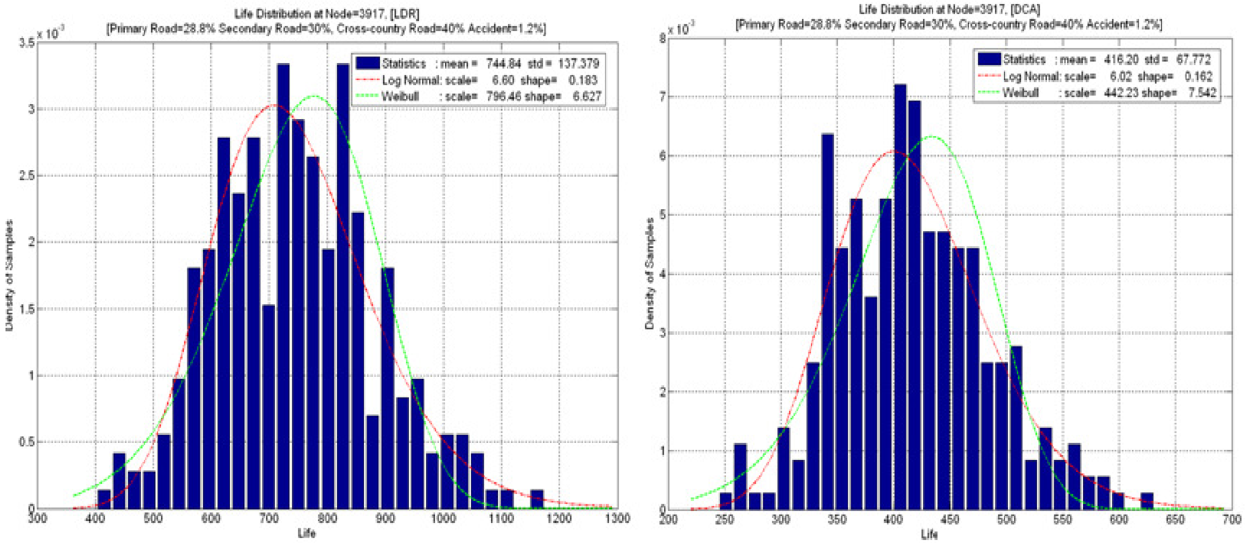

Figure 16 Predicted FLSS Life Usind LDR and DCA Progressive Damage Models

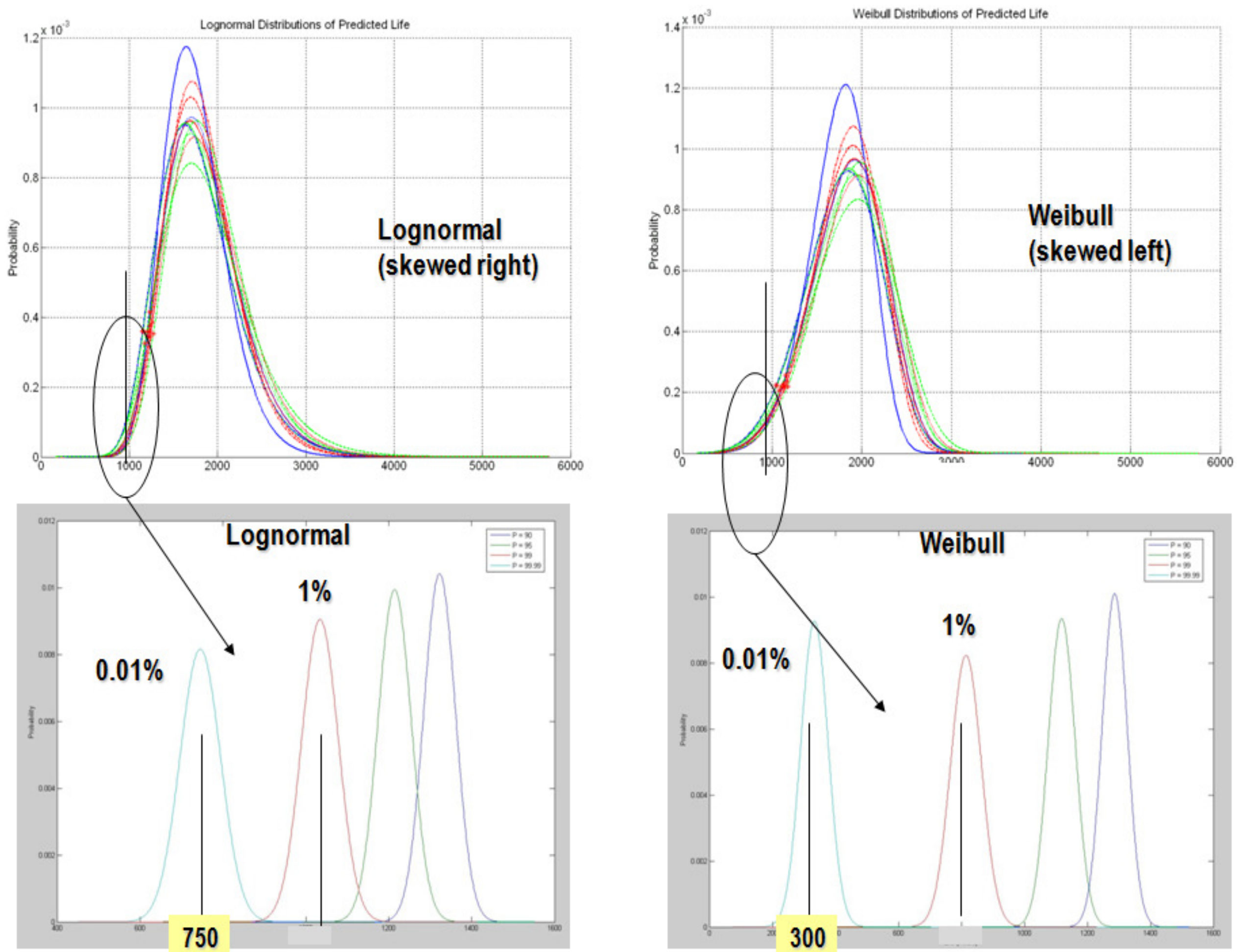

Figure 17 Effect of Lack of Data (280 Simulations) on Predicted Life for Given Reliability Levels of 90%, 95%, 99% and 99.99%

CONCLUSIONS

To efficiently and accurately solve the challenges of vehicle reliability predictions coming from using large-size computational mechanics models in high-dimensional stochastic parameter spaces, an integrated HPC-based stochastic simulation based reliability approach was developed and implemented.

The integrated reliability approach includes innovative tools that provide a great efficiency to the overall HPC implementation. These tools include advanced stochastic process models to describe the road profiles, stochastic FE techniques for domain decomposition and stochastic preconditioning fast MCMC simulation, three-level hierarchical and meshless probability integration models for stochastic response approximation and simulation, enhanced Bayesian model updating schemes, and an efficient Bayesian framework for incorporating modeling uncertainties and lack of data, and computing variation bounds (confidence intervals) of predicted risks.

The integrated vehicle fatigue reliability prediction approach incorporates the following steps:

i) simulation of the stochastic operational environment,

ii) stochastic vehicle multi-body dynamics analysis,

iii) stress prediction in subsystems and components,

iv) stochastic progressive damage analysis, and

v) component life prediction, eventually including off-line maintenance and on-line monitoring

vi) reliability prediction at vehicle component and system levels.

The new integrated reliability approach is illustratively applied to predict the HMMWV suspension system probablistic life and reliability. The paper shows that a accurate stochastic modeling of road surface and topography variations are important aspects of an overall vehicle reliability analysis. Road surface variations are highly non-Gaussian, being rightly-skewed toward larger amplitudes. The non-Gaussian variation aspects of the road profiles have a significant impact on the predicted vehicle fatigue reliability. This is an important reliability aspect that was ignored in practice for long time.

The paper also shows that the progressive damage modeling and the effect of limited simulation data impacts significantly on the HMMWV suspension system reliability prediction.

ACKNOWLEDGEMENTS

The authors would like to thank to Justin Madsen, graduate student at University of Wisconsin at Madison, who performed a large number of HMMWV ADAMS simulations. We also acknowledge the DOD SBIR funding support for GP Technologies, Inc. and University of Wisconsin at Madison under the DOD SBIR A06-224 topic.

REFERENCES

[1] Gipser, M. "FTire: a physically based application-oriented tyre model for use with detailed MBS and finite-element suspension models." Vehicle Systems Dynamics 43 Supplement: 76 - 91, 2005

[2] Aardema, J. “Failure analysis of the lower rear ball joint on the High-Mobility Multipurpose Wheeled Vehicle.” U.S. Army Tank-Automotive Command Technical Report # 13337, Warren, MI, 1988

[3] Ghiocel, D.M., Lamb, D. and Hudas, G.,"Advances in Computational Stochastic Mechanics and Reliability Prediction for Ground Vehicles", 2007 SIAM Conference "Mathematics for Industry", October 2007

[4] Ghiocel, D.M. and Tuegel, E., "Reliability Assessment of Aircraft Structure Joints Under Corrosion-Fatigue Damage", *Engineering Design Reliability Applications: For the Aerospace, Automotive and Ship Industries*", eds. Nikolaidis, Ghiocel and Singhal, CRC Press, September 2007

[5] Ghiocel, D. M. "Advances in Computational Risk Predictions for Complex, Large Size Structural Engineering Applications" *46th AIAA/ASME/ASCE/AHS/ASC Structures, Structural Dynamics & Material Conference*, AIAA-2005-2222, Austin, TX, April 18-21, 2005

[6] Ghiocel, D.M.,"Stochastic Simulation Methods for Engineering Predictions", *Chapter 20 in "Engineering Design Reliability Handbook"*, eds. Nikolaidis, Ghiocel and Singhal, CRC Press, December, 2004

[7] Madsen, J, Ghiocel, D.M., Lamb, D., Gorsich, D. and Negrut, D., "A Stochastic Approach to Integrated Vehicle Reliability Prediction", Proceedings of the ASME 2009 International Design Engineering Technical Conferences & 7th International Conference on Multibody Systems, Nonlinear Dynamics, and Control, IDETC/MSNDC, 2009